Bilateral asymmetry identification for the early detection of breast cancer

A. Mencattini, M. Salmeri, P. Casti
Dept. of Electronic Engineering
University of Rome Tor Vergata, Rome, Italy
Email: {mencattini,salmeri}@ing.uniroma2.it,paola_casti85@hotmail.com

***Abstract*—Breast cancer is the second most common cancer overall and the leading cause of cancer deaths in women. Mammography is, at present, the only viable method for detecting most of tumors early enough for effective treatment. The secret of setting up the accurate diagnosis is to detect and understand the most subtle signs of breast lesions. Analysis of asymmetry between the left and right mammograms can provide clues about the presence of early signs of tumors. In this work we present an automated procedure for bilateral asymmetry detection composed of the following steps: (1) mammography density analysis and fibro-glandular disc detection through adaptive clustering techniques, (2) analysis and implementation of bilateral asymmetries detection algorithms based on Gabor filters analysis, (3) use of a linear Bayes classifier with the leave-one-out method to asses the asymmetry degree of the two breasts, (4) metrological evaluation of the whole system through random and systematic measurement uncertainty contributions modeling.**

I. Introduction

Breast cancer is the second most common cancer overall and the most prevalent cancer among women. Based on recent statistics from the International Agency for Research on Cancer [1], breast cancer account for 10.9% of all cancers diagnosed and ranks as the fifth cause of cancer death in the world. Although incidence rates are increasing, mortality rates are stable, representing an improved survival rate. This improvement can be attributed to effective means for the early detection as well as to significant improvement in treatment options, exposure, etc. Mammography is, at present, the only viable method for detecting most of tumors early enough for effective treatment, without unnecessary biopsies or other invasive procedures. Therefore, screening mammography in women aged 40 to 70 years is currently the effective strategy to reduce breast cancer mortality. Early detection of invasive breast cancers is associated with better prognosis than waiting for women to become symptomatic. However, detecting the early signs of breast cancer is challenging because the cancerous structures have many features in common with normal breast tissue. Moreover, the accuracy of interpretation of screening mammograms is affected by several factors, such as image quality, the radiologist's level of expertise, and the high volume of cases. According to recent statistics, in current breast cancer screenings, $10\% - 25\%$ of the tumors are missed by the radiologists. Computer Aided Detection (CADe) systems can support radiologists in the role of a second reader [2], aiding the radiologist in finding the suspicious breast lesions and distinguishing between what is decidedly negative on a mammogram, as opposed to what needs regular monitoring and what requires a needle biopsy. The secret of setting up the accurate diagnosis is to detect and understand the most subtle signs of breast lesions [3]. According to the fourth edition of Breast Imaging Reporting and Data System (BIRADS) [4], subtle signs of breast cancer are four: calcifications, masses, architectural distortion, and bilateral asymmetry. The latest two signs do not necessarily mean that cancer is already present, but provide clues about the presence of early signs of tumors. However, a few works have been reported on the detection of bilateral asymmetry. It may be due to the fact that bilateral asymmetries are difficult to be identified because they need a comparison among left and right views of the two breasts, that is a very difficult task owing to the natural diversity among breast skin line, orientation, manual position of the breast during X-ray exposure, etc. In this work, we present a procedure for bilateral asymmetry detection composed of the following steps: (1) mammography density analysis and fibro-glandular disc detection through adaptive clustering techniques, (2) analysis and implementation of bilateral asymmetries detection algorithms based on Gabor filters analysis, (3) use of a linear Bayes classifier with the leave-one-out method to asses the asymmetry degree of the two breasts, (4) metrological validation of the whole system through the modeling of the uncertainty contributions estimated in the specific context.

II. Bilateral asymmetry

Asymmetry between the left and right mammograms of a given subject is an important sign used by radiologists to diagnose breast cancer. Analysis of asymmetry can provide clues about the presence of early signs of tumors like parenchymal distortion, small asymmetric bright spots and contrast, that are not evaluated by other methods [3]. Tumor-related-asymmetries are those that are changing, enlarging, those that are palpable or associated with other findings, such as microcalcifications and architectural distortion [5]. Lau and Bishof [6] proposed a method for detection of breast tumors using the asymmetry principle, through measures of brightness, roughness, and directionality. The method was tested with a set of ten mammograms pairs where asymmetry was significant for the radiologist's diagnosis. A sensitivity of 92% was obtained with 4.9 false positives per mammogram. Miller and Astley [7] implemented a semiautomated texture-based

978-1-4244-9338-8/11/$26.00 ©2011 IEEE

procedure for the segmentation of the glandular tissue and measures of shape and grey level distribution for the detection of asymmetry. An accuracy of 86.7% was reported with a test dataset of 30 screening mammogram pairs. In another report [8], the same authors presented a method based on measures of shape, brightness and topology of the fibro-glandular disc. The method was tested on 104 mammograms pairs and a classification accuracy of 74% was obtained. Ferrari et al. [5] used directional filtering with Gabor wavelets. In their method, which was applied only to MLO views, the fibro-glandular disc is segmented and the resulting image is decomposed using a bank of Gabor filters at 12 orientations and four scales. The Karhunen-Loeve transform is employed to select the principal components of the filters responses. Variations in oriented textural patterns are detected from the difference in rose diagrams of the phase images and additional set of features are extracted from the fibro-glandular disc. A database of 80 images containing 20 normal cases, 14 asymmetric cases, and six architectural distortion cases was used to evaluate the algorithm. The authors reported classification accuracy rates of up to 74.4%. Rangayyan et al. [9] extended the method of Ferrari et al. by including morphological measures to quantify differences in fibro-glandular-tissue-covered areas in the left and right breasts, which relate to size and shape; in addition, the directional data were aligned with reference to the edge of the pectoral muscle (in MLO views). A sensitivity of 82.6% and a specificity of 86.4% were obtained in the detection of bilateral asymmetry with a set of 88 mammograms. In the following sections we describe in detail a procedure for the detection of bilateral asymmetry and a sketch of the algorithm validation.

III. The database

This preliminary study has been developed using Screen Film Mammographic images (SFM) from the Mini-MIAS Database [10] originally digitized at a spatial resolution of 50 μm and then reduced to 200 μm and 8 bpp. The images include 22 normal cases and 22 abnormal cases (15 asymmetries and 7 architectural distortions).

IV. The proposed methodology

The proposed method is schematized in Fig. 1 and it is composed of the following steps:

A. breast skin profile identification and pectoral muscle line orientation extraction;
B. contrast enhancement;
C. segmentation of the fibro-glandular disc;
D. extraction of the oriented pattern in the fibro-glandular tissue;
E. alignment of the left and right discs according to the pectoral muscle line orientation;
F. features extraction;
G. pattern classification for the bilateral asymmetry identification.

Let us see in details the principal issues regarding the steps outlined above.

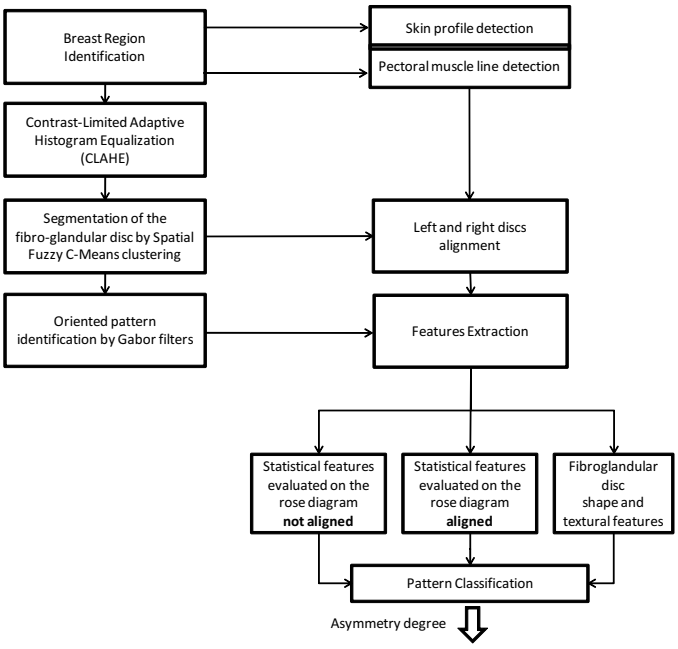

Fig. 1. A schematic flowchart of the whole algorithm.

A. Breast region identification

The first issue addressed in our procedure is the segmentation of the breast parenchyma from the rest of the image. In the Medio-Lateral Oblique views (MLO) the procedure is composed of two stages: the first step extracts the breast region from the rest of the image (background) using an active contour algorithm, the second step suppresses the pectoral muscle using histogram thresholding and Hough transform [11]. An example of the result is shown in Fig. 2(b).

B. Contrast Enhancement

The contrast enhancement of the images is done using the Contrast Limited Adaptive Histogram Equalization (CLAHE) technique, which is a special case of the histogram equalization technique that functions adaptively on the image to be enhanced, preventing over enhancement of noise and reducing the edge-shadowing effect [12]. Fig. 2(c) shows a MLO view of the mammogram after contrast enhancement.

C. Segmentation of the fibro-glandular disc

In the bilateral asymmetry evaluation, only the fibro-glandular disc is usually used, as the Region Of Interest (ROI), in order to compute the oriented components; this is due to the fact that most of the directional components, such as connective tissues and ligaments, exists in this specific region of the breast [13]. Our method uses an adaptive Spatial Fuzzy-C-Means (SFCM) clustering, which is an improvement of the FCM algorithm that incorporates spatial information reducing the effect of noise and biasing the algorithm toward homogeneous clustering [14].

Considering a set of N data $\{x_i\}$, $i = 1, \ldots, N$, a set of C classes $\{c_j\}$, $j = 1, \ldots, C$, and any real number $m > 1$, the

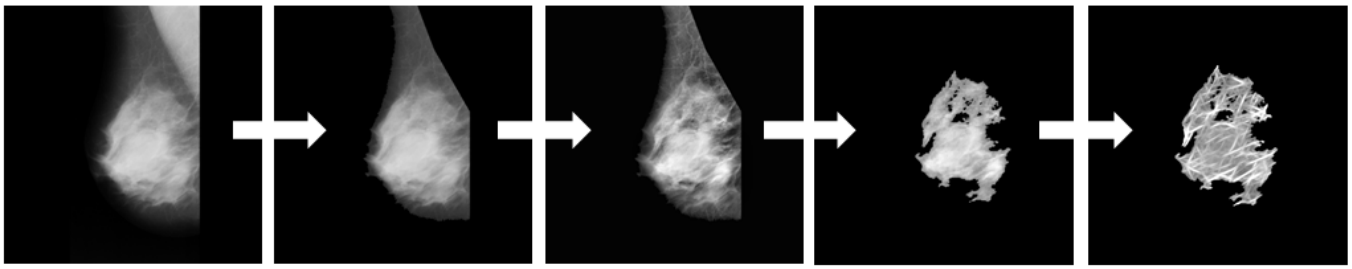

Fig. 2. Steps for the segmentation and evaluation of the fibro-glandular disc. (a)-(e)

method is based on the minimization of the objective function

$$J_m = \sum_{i=1}^{N}\sum_{j=1}^{C} u_{ij}^m \|x_i - c_j\|^2, \quad 1 \le m < \infty$$

where u_{ij} is the degree of membership of x_i to the cluster j, and $\|\cdot\|$ represents any norm able to represent similarity among any measured data and the center. Fuzzy partitioning is achieved by an iterative optimization procedure where at each step u_{ij} and c_j are updated as follows

$$u_{ij} = \frac{1}{\sum_{k=1}^{C}\left(\frac{\|x_i - c_j\|}{\|x_i - c_k\|}\right)^{\frac{2}{m-1}}}, \qquad c_j = \frac{\sum_{i=1}^{N} u_{ij}^m \cdot x_i}{\sum_{i=1}^{N} u_{ij}^m}$$

Furthermore, one of the important characteristics of an image is that neighboring pixels are highly correlated. This spatial relationship is not utilized in the conventional FCM algorithm, where the noise can lead to a misclassification. To reduce the effect of noise in [14] the authors apply a spatial FCM algorithm to breast segmentation in ultrasound images, by altering the membership weighting of each cluster. So, the new spatial membership degrees become

$$u'_{ij} = \frac{u_{ij}^p \cdot f^q(u_{ij})}{\sum_{k=1}^{C} u_{ik}^p f^q(u_{ik})}$$

where $f(u)$ is a spatial weight function here defined as the median filter apply to the image of membership degrees u_{ij}, while p and q are parameters to control the relative importance of u and f terms. In our setting, we choose $p = 0.1$ and $q = 0.9$. The iterations stop when $\max|u_{ij}^{'k+1} - u_{ij}^{'k}| < \epsilon$ for a given $\epsilon \in (0, 1]$). When the procedure stops rows of matrix $U = \{u_{ij}\}$ contain the membership degree of each element x_i to every class c_j. A final decision is taken considering for example the maximum membership degree for each x_i.

This procedure allows us to roughly grouping pixels inside the image belonging to the fibro-glandular disc. The key point is the choice of the number of classes in the SFCM algorithm that, to our experience, should depend on the breast density. Our model uses the hypotheses that the number of classes in the effective region of the breast can vary from two to four according to the density assessment in BIRADs: uncompressed fatty tissues, fatty tissues, non-uniform density tissues, high density tissues. We have investigated the use of validity measures like the *Classification Entropy* that measures the fuzzyness of the cluster partition [15], the *Partition Index* that represents the ratio of the sum of compactness and separation of the clusters [16], the *Separation Index* that uses a minimum-distance separation for partition validity [16], and finally the Dunn's Index, an identifier of "compact and well separated clusters" and the simplified Alternative Dunn's Index [17]. At the moment the final number of classes is chosen considering the minimum value reached by the sum of the above metrics. Fig. 2(d) shows the fibro-glandular disc extracted using the SFCM algorithm using 2 classes.

D. Gabor filters for the extraction of the oriented pattern in the fibro-glandular disc

At present, the most innovative technique described in the literature to evaluate bilateral asymmetry has been developed by Rangayyan [9]. The method implements a directional analysis using a multiresolution approach based on Gabor wavelets. Following an analogous procedure, here we propose the use of Gabor filters with a single scale related to the average width of fibro-glandular tissue [18]. 2D Gabor filters are a category of filters obtained from a sinusoidal plane wave of some frequency and orientation within a two dimentional Gaussian envelope. The real Gabor filter kernel oriented at the angle $\theta = -\pi/2$ is given by

$$g(x, y) = \frac{1}{2\pi\sigma_x\sigma_y}\exp\left[-\frac{1}{2}\left(\frac{x^2}{\sigma_x^2} + \frac{y^2}{\sigma_y^2}\right)\right]\cos(2\pi f x)$$

Filters at other angles are obtained by rotating this kernel over the range $[-\pi/2, \pi/2]$ by the angles $\alpha_k = -\pi/2 + \pi k/180$, $k = 0, 1, \ldots, 180 - 1$. Letting τ be the full-width at half-maximum of the Gaussian term, the parameters of the Gabor filter kernel are defined as follows: $\theta_x = \tau/(2\sqrt{2\ln 2})$, $\theta_y = l\theta_x$ and $f = 1/\tau$. In this work we use $l = 8$ and $\tau = 3$ for 180 equally spaced filters over the angular range defined above, obtaining a bank of real Gabor filters from which the Gabor-filtered images $W_k(x, y)$ are calculated. The resulting orientation field is given by the angle

$$\phi(x, y) = \alpha_{k_{max}}, \quad k_{max} = arg\{\max_k[W_k(x, y)]\}$$

and by the magnitude of the output of the real Gabor filter at the optimal orientation. In Fig. 2(e) the Gabor magnitude inside the fibro-glandular tissue, obtained after the directional analysis, is shown.

Fig. 3 reports two preliminary examples of the fibro-glandular disc extraction for asymmetric and normal cases from Mini-MIAS database, showing the original images and the Gabor magnitude of the extracted fibro-glandular discs. Fig. 4 shows the associated rose diagrams, representing the angular distribution of the oriented tissue extracted from the Gabor filters analysis of both the right and the left breasts in the same projection.

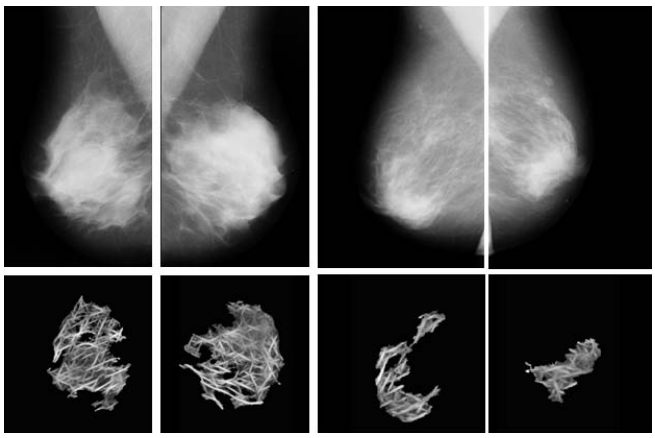

Fig. 3. Example of a normal and an asymmetric case and the Gabor magnitude of the fibro-glandular discs

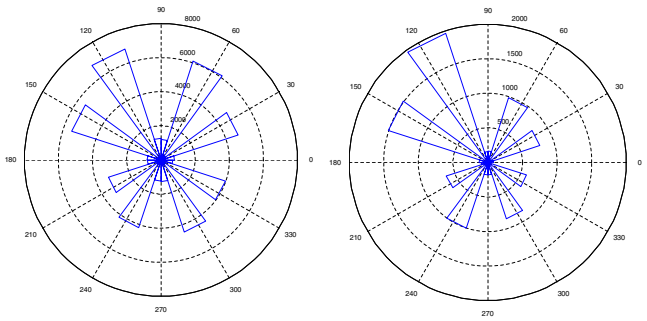

Fig. 4. Rose diagrams for a normal and an asymmetric case.

Note that the rose diagram exhibits a symmetric angular distribution for the normal case, while it is strongly asymmetric when bilateral asymmetry is present.

E. Alignment of fibro-glandular discs

Denote with δ the difference among the left and the right pectoral muscle line orientations, after performing a proper mapping of the left image on the right one. This angle is used to correct the angular distribution of the fibro-glandular discs taking into account the pectoral muscle orientation. One example is reported in Fig. 5.

F. Features extraction

Starting from the difference rose diagrams (obtained subtracting the two rose diagrams of the left and right mammograms) and from the fibro-glandular discs, the extraction of

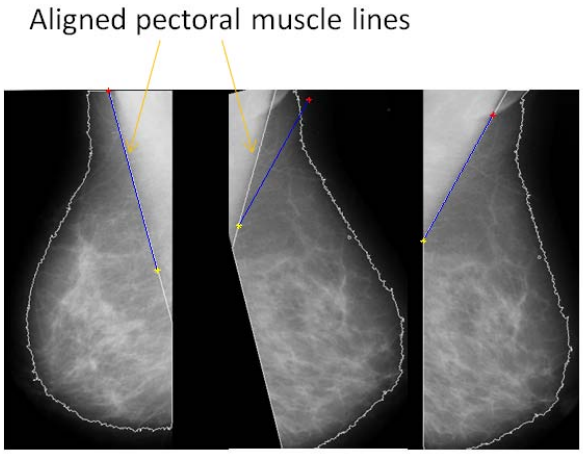

Fig. 5. Example of the alignment procedure accounting for the lack of symmetry between the pectoral muscle line orientations.

the most relevant features to detect the regions of asymmetry in the breast can be divided into four steps.

1) Compute statistical features on the difference rose diagrams [9].
2) Compute morphological measures and geometric moments of the segmented fibro-glandular discs.
3) Select the most relevant features using the modified stepwise regression procedure described in [19].
4) Perform the principal component analysis (PCA) [20] to transform the selected features into uncorrelated variables.

At present, the following features have been computed:

i) Entropy H, first, and second angular moments of the difference of the two rose diagrams M_1 and M_2, dominant orientation θ_R, and circular variance s_θ^2, defined in [9]: these parameters relate to the angular distribution in the residual rose diagram taking into account for the statistical angular difference among left and right fibro-glandular discs. The parameters are not evaluated on the aligned rose diagrams.

ii) The same features in i) but evaluated on the rose diagrams aligned according to δ.

iii) The seven Hu's moments [21] $\phi_1, \ldots, \phi_7$ used to quantify the difference of the shape and of the texture in the two fibro-glandular discs.

iv) The difference of eccentricity, stretch parameter, density, and area of the two fibro-glandular discs [9].

G. Pattern classification for the bilateral asymmetry identification

In order to assess the asymmetry degree of the two breasts we use a classifier that, according to the selected features, assigns to the patient the probability of the presence of a bilateral asymmetry. The leave-one-out methodology is used to estimate the classification accuracy because the number of samples is relatively small, while classification is performed using a linear Bayes classifier [20].

	Sensitivity	Specificity
H not aligned	0.68	0.77
M_1 not aligned	0.73	0.64
M_2 not aligned	0.68	0.73
s^2 not aligned	0.72	0.82
Eccentricity	0.54	0.54
ϕ_1	0.54	0.59

TABLE I
RESULTS OF THE UNIVARIATE ANALYSIS. ONLY THE MOST SIGNIFICANT FEATURES ARE SHOWN.

V. RESULTS

In this study, we only report preliminary results related to the fibro-glandular discs segmentation, the characterization of the two angular distributions, and the features extraction. Future works will address the problem of asymmetry assessment.

In particular, an univariate analysis has been performed to evaluate the performance of each feature for the asymmetry assessment, in terms of *Sensitivity* and *Specificity*

$$\textit{Sensitivity} \doteq \frac{TP}{TP+FN} \qquad \textit{Specificity} \doteq \frac{TN}{TN+FP}$$

where:

- TP (True Positive) is the pair of mammograms where an expert radiologist has reported an asymmetry in the left or in the right breast and the algorithm does the same;
- FP (False Positive) is the pair of normal mammograms that the algorithm marks as asymmetric;
- TN (True Negative) is the pair of normal mammograms that the algorithm marks as normal;
- FN (False Negative) is the pair of mammograms in which an expert radiologist identifies an asymmetry and the algorithm marks as normal.

Tab. I reports the sensitivity and the specificity of the most significant features. Preliminary results are obtained performing a stepwise regression analysis followed by a PCA of the selected features from the 21 identified, for the 44 pairs of images taken from the Mini-MIAS database. The pattern classification step has been performed using a linear Bayes classifier thus obtaining: *Sensitivity* $= 0.82$ and *Specificity* $= 0.82$.

VI. METROLOGICAL VALIDATION

The metrological validation of the whole procedure is based on the propagation of all the uncertainty contributions through the blocks of the algorithm. Suitable methods have to be implemented according to the typologies of blocks considered. For direct or iterative computational blocks a Monte Carlo simulation is recommended [22], while for the propagation of random contributions through rule-based systems novel approaches recently developed by Ferrero [23] and later applied in [24] are more suited.

An exhaustive validation procedure should face the following aspects:

- UNCERTAINTY ESTIMATION. Three uncertainty contributions can be outlined:
  i) the pixel depth in the range $[8 - 16]$ *bpp*;
  ii) the image power noise, estimated by specific algorithms [25], tailored for heteroscedastic noise contributions (noise variance changes with luminance);
  iii) the tolerance in the identification of the pectoral muscle orientation affecting the computation of aligned features.
- UNCERTAINTY PROPAGATION. The output of this step provides an interval of confidence around the asymmetry degrees produced by the classifier, taking into account uncertainty contributions i)-iii).

In this study, we have performed an analysis of sensitivity of the aligned features and of the final asymmetry assessment performance, with respect to contributions iii). Future works will consider the other uncertainty contributions and their propagation.

In particular, a Monte Carlo simulation has been developed thus producing the trend of the sensitivity and of the specificity of the aligned features H, M_1, M_2, θ_R, and s^2_θ versus the pectoral muscle line orientation varying the δ of the alignment among left and right rose diagrams around its nominal value δ^0 in the range $[\delta^0 - 5^\circ,\ \delta^0 + 5^\circ]$ with a step of 0.5°. Results of the sensitivity analysis are reported in Fig. 6. A Monte Carlo

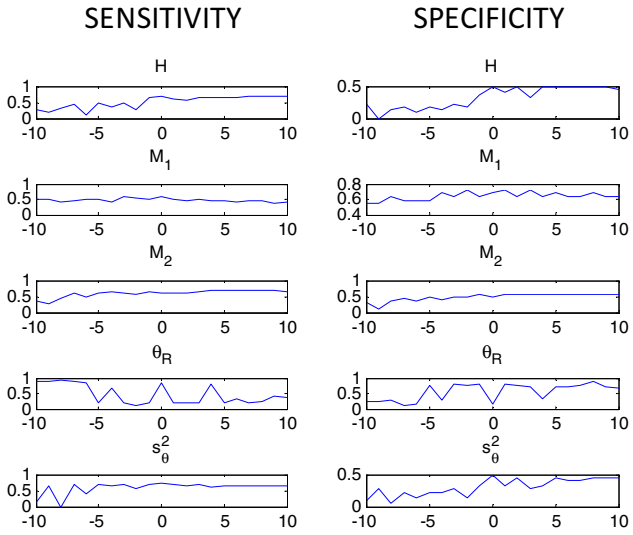

Fig. 6. Sensitivity and specificity of aligned features varying the alignment angle δ related to the difference between the two pectoral muscle line orientations.

simulation has been then implemented in order to extract the distribution of the sensitivity and of the specificity of the final assessment procedure, varying the alignment angle and considering only features H, M_1, M_2, θ_R, and s^2_θ. Numerical results are reported in Tab. II while the cumulative distribution of the sensitivity and of the specificity along with the confidence bounds associated to level of confidence 90%, 80%, 70% are reported in Fig. 7.

	Sensitivity		Specificity	
$I_{90\%}$ - Mean	[0.701 1.000]	0.778	[0.571 0.886]	0.743
$I_{80\%}$ - Mean	[0.703 0.966]	0.778	[0.596 0.872]	0.743
$I_{70\%}$ - Mean	[0.709 0.936]	0.778	[0.619 0.856]	0.743

TABLE II
CONFIDENCE INTERVALS AND MEAN VALUE FOR SENSITIVITY AND SPECIFICITY AFTER THE PATTERN CLASSIFICATION STEP, VARYING THE PECTORAL MUSCLE LINE ORIENTATION

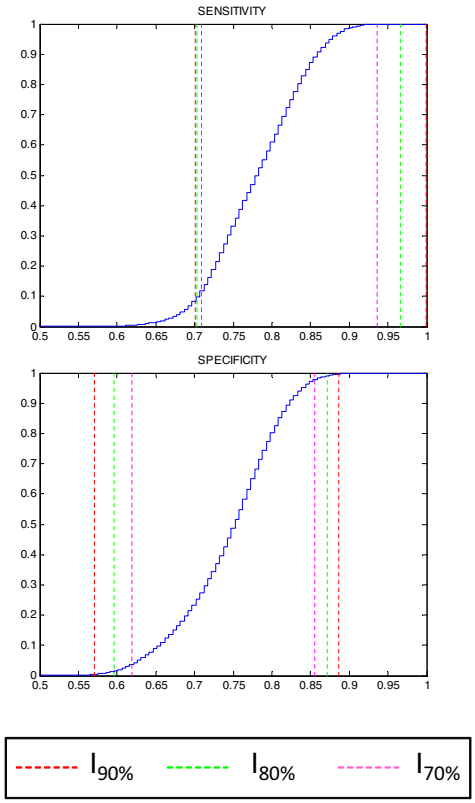

Fig. 7. Cumulative distribution for the sensitivity and the specificity along with the confidence bounds for three confidence levels 90%, 80%, 70%

VII. CONCLUSIONS

In this study, preliminary results of a novel methodology regarding the automatic bilateral asymmetry identification in mammograms have been reported. The whole methodology has been described and a sketch of the metrological validation has been provided. An analysis of sensitivity has been also included considering the tolerance in the determination of the alignment angle which corresponds to the difference between the left and right pectoral muscle line orientations. A preliminary pattern classification procedure has been also implemented, providing the results in terms of sensitivity and specificity along with their confidence intervals for various confidence levels varying the alignment angle.

REFERENCES

[1] J. Ferlay et al., "Estimates of worldwide burden of cancer in 2008: Globocan 2008," *International Journal of Cancer*, vol. 127, pp. 2893 – 2917, 2010.

[2] M. Bazzocchi et al., "Cad systems for mammography: a real opportunity? a review of the literature," *Radiol. Med.*, vol. 112, pp. 329 – 353, 2007.

[3] V. Lattanzio and G. Simonetti, *Mammography-guide to interpretation, reporting and auditing mammographic images Re. Co. R. M.*, Springer-Verlag, 2007.

[4] C. Balleyguier et al., "Birads^{TM} classification in mammography," *European Journal of Radiology*, vol. 61, pp. 192 – 194, 2007.

[5] R.J. Ferrari, R.M. Rangayyan, J.E.L. Desautels, and A.F. Frere, "Analysis of asymmetry in mammograms via directional filtering with gabor wavelets," *IEEE Transactions on Medical Imaging*, vol. 20, no. 9, pp. 953 – 964, 2001.

[6] T.K. Lau and W.F. Bischof, "Automated detection of breast tumors using the asymmetry approach," .

[7] P. Miller and S. Astley, "Detection of breast asymmetry using anatomical features," in *Biomedical Image Processing and Biomedical Visualization, Proceedings of SPIE*, C.B. Goldgof R.S. Acharya, Ed., 1993, vol. 1905, pp. 433 – 442.

[8] P. Miller and S. Astley, *Automated detection of breast asymmetry using anatomical features*, vol. 9 of *Series in Machine Perception and Artificial Intelligence*, chapter State of the Art in Digital Mammographic Image Analysis,, pp. 433 – 442, World Scientific, River Edge, NJ, 1994.

[9] R. J. Ferrari R. M. Rangayyan and A. F. Frere, "Analysis of bilateral asymmetry in mammograms using directional, morphological, and density features," *J. Electron. Imag.*, vol. 16, no. 1, 2007.

[10] J. Suckling et al., "The mammographic image analysis society digital mammogram database," in *Proc. 2nd Int. Workshop Digital Mammography*, D. R. Dance A. G. Gale, S. M. Astley and Eds. A. Y. Cairns, Eds., York, U.K., 1994, pp. 375 – 378.

[11] A. Mencattini et al., "Features extraction and fuzzy logic based classification for false positives reduction in mammographic images," in *International Conference on Bio-inspired Systems and Signal Processing (BIOSIGNALS '11)*, Rome, Italy, Jan 2011.

[12] E.D. Pisano et al., "Contrast limited adaptive histogram equalization image processing to improve the detection of simulated spiculations in dense mammograms," *Journal of Digital Imaging*, vol. 11, no. 4, pp. 193 – 200, 1998.

[13] R.J. Ferrari et al., "Segmentation of the fibro-glandular disc in mammograms using gaussian mixture modeling," *Medical Biology Engineering Computing*, vol. 42, pp. 378 – 387, 2004.

[14] Y. Xu and T.Nishimura, "Segmentation of breast lesions in ultrasound images using spatial fuzzy clustering and structure tensors," *Medical Biology Engineering Computing*, vol. 53, 2009.

[15] J. C. Bezdek, *Pattern Recognition with Fuzzy Objective Function Algorithms*, Plenum Press, 1981.

[16] A.M. Bensaid et al., "Validity-guided (re)clustering with applica- tions to imige segmentation," *IEEE Transactions on Fuzzy Systems*, vol. 4, pp. 112 – 123, 1996.

[17] T.C. Havens, J.C. Bezdek, J.M. Keller, and M. Popescu, "Dunns cluster validity index as a contrast measure of vat images," in *Proc ICPR*, Tampa, FL, 2008.

[18] Fbio J. Ayres and R. M. Rangayyan, "Design and performance analysis of oriented feature detectors," *Journal of Electronic Imaging*, vol. 16, no. 2, 2007.

[19] P.C. Austin and J. Tu, "Bootstrap methods for developing predictive models," *Am. Statistician*, vol. 58, pp. 131 – 137, 2004.

[20] R.O. Duda and P.E. Hart, *Pattern classification and scene analysis*, Wiley-New York, 1973.

[21] M.K. Hu, "Visual pattern recognition by moment invariants," *IRE Trans. Inf. Theory*, vol. 8, no. 2, pp. 179 – 187, 1962.

[22] JCGM, "Evaluation of measurement data - an introduction to the guide to the expression of uncertainty in measurement 104:2009," Tech. Rep., JCGM, 2009.

[23] A. Ferrero, A. Federici, and S. Salicone, "A method for considering and processing measurement uncertainty in fuzzy inference systems," in *International Instrumentation and Measurement Technology Conference (I2MTC 2009)*, May 2009, pp. 5 – 7.

[24] A. Ferrero et al., "Uncertainty evaluation in a fuzzy classifier for microcalcifications in digital mammography," in *IEEE Instrumentation and Measurement Technology Conference (IMTC '10)*, Austin, TX, USA, May 2010.

[25] M. Salmeri, A. Mencattini, G. Rabottino, and R. Lojacono, "Signal-dependent noise characterization for mammographic images denoising," in *IMEKO TC4 Symposium*, Firenze, Italy, 2008.